Title: Spectral diversity in default mode network connectivity reflects behavioural state.

Short title: Task-related high frequency connectivity in DMN

Authors: Michael M Craig[1,2], Anne E Manktelow[1,2], Barbara J Sahakian[3], David K Menon[1,2], Emmanuel A Stamatakis[1,2]

Author Affiliations:

1) Division of Anaesthesia, Department of Medicine, School of Clinical Medicine, University of Cambridge, Cambridge, United Kingdom
2) Wolfson Brain Imaging Centre, Department of Clinical Neurosciences, School of Clinical Medicine, University of Cambridge, Cambridge, United Kingdom
3) Department of Psychiatry, School of Clinical Medicine, University of Cambridge, Cambridge, United Kingdom

Corresponding Author:
Michael M Craig
Division of Anaesthesia and Department of Clinical Neurosciences
School of Clinical Medicine, University of Cambridge
Box 93, Addenbrooke's Hospital, Hills Road, Cambridge CB2 0QQ, UK
Email: mmc57@cam.ac.uk

Keywords: Bandpass filtering; Default Mode Network; Dorsal attention network; Internetwork Connectivity; Anticorrelations

Author Email Addresses:

Anne E Manktelow	am807@cam.ac.uk
Barbara J Sahakian	bjs-sec@medschl.cam.ac.uk
David K Menon	dkm13@wbic.cam.ac.uk
Emmanuel A Stamatakis	eas46@cam.ac.uk

Abstract

Default mode network (DMN) functional connectivity is thought to occur primarily in low frequencies (< 0.1 Hz), resulting in most studies removing high frequencies during data preprocessing. In contrast, subtractive task analyses include high frequencies, as these are thought to be task relevant. An emerging line of research explores resting fMRI data at higher frequency bands, examining the possibility that functional connectivity is a multi-band phenomenon. Furthermore, recent studies suggest DMN involvement in cognitive processing, however without a systematic investigation of DMN connectivity during tasks, its functional contribution to cognition cannot be fully understood. We bridged these concurrent lines of research by examining the contribution of high frequencies in the relationship between DMN and dorsal attention network (DAN) at rest and during task execution. Our findings revealed that the inclusion of high frequencies alters between network connectivity resulting in reduced anticorrelation and increased positive connectivity between DMN and DAN. Critically, increased positive connectivity was observed only during tasks suggesting an important role for high frequency fluctuations in functional integration. Moreover, within DMN connectivity during task execution correlated with reaction time only when high frequencies were included. These results show that DMN does not simply deactivate during task execution and suggest active recruitment while performing cognitively demanding paradigms.

1. Introduction

Large scale brain networks form a complex system of connections capable of supporting a wide range of behaviours. Using functional magnetic resonance imaging (fMRI) multiple brain networks have been consistently identified using a variety of statistical techniques (Damoiseaux et al., 2006; Smith et al., 2009). Many of these networks have substantial overlap with brain areas important to various tasks, suggesting the collective activity of the network mediates exteroceptive attention (Dosenbach et al., 2007). The default mode network (DMN), despite initial studies suggesting it deactivates during externally driven tasks (Shulman et al., 1997; Mazoyer et al., 2001), has recently been shown to play a crucial role in a variety of introspective and attentionally demanding tasks (Buckner and Carroll, 2006; Vatansever et al., 2015a; Vatansever et al., 2016). This includes interoceptive attentional processes such as autobiographical memory, prospective memory, moral judgement and theory of mind (Buckner et al., 2008; Spreng and Grady, 2010; Andrews-Hanna, 2012; Spreng et al., 2013) as well as attentionally demanding executive function tasks (Vatansever et al., 2015b).

A recurrent element in brain network studies is that network fluctuation is maximally observed at low frequencies; therefore most researchers bandpass filter their data prior to statistical analysis, typically retaining frequencies above ~0.01Hz and below ~0.1Hz (Biswal et al., 1995; Greicius et al., 2003; Fransson et al., 2005; Fox et al., 2005; Murphy et al., 2013). While it is true that most statistical power is contained within these low frequencies, recent work has shown that higher frequencies (those above 0.1Hz) also contain non-noise signal (Kalcher et al., 2014). Highpass filtering is relatively uncontroversial, as it removes low frequency drifts due to scanner noise. However lowpass filtering has been shown to be problematic in that it decreases sensitivity to task-related activations without increasing specificity (Skudlarksi et al., 1999; Della Maggiore et al., 2002) and induces spurious autocorrelation in resting state studies (Davey et al., 2013). Furthermore, recent work has found that many artefactual signals have spectral peaks within the low frequencies used to identify large scale networks or are aliased into these frequencies by the low sampling rate of fMRI (Birn et al., 2008; Van Dijk et al. 2010). Recently these problems have been dealt with through novel denoising statistical techniques like anatomical CompCor (Behzadi et al., 2007; Chai et al., 2012), in which

principle components from noise regions of interest and movement parameters and their first derivatives are removed.

There is a small but growing body of literature focused on understanding high frequency contributions to functional connectivity measures. (Wu et al., 2008; Niazy et al., 2011; Boyacioglu et al., 2013; Gohel and Biswal, 2014; Kalcher et al., 2014; Chen and Glover, 2015; De Domenico et al., 2016; Lewis et al., 2016). A recent study by Chen and Glover (2015) collected resting state data at different echo times (TE) to examine the relative contributions of BOLD and non-BOLD components to resting state connectivity at different time scales. Their study focused on connectivity in DMN and the executive control network (a subnetwork of the DAN) and found altered spatial patterns at different frequency bands. Notably, they found that some subjects showed anticorrelations between DMN and executive control network only in low frequencies. These connections became positive when sampled between 0.2-0.4 Hz suggesting that anticorrelations between DMN and DAN, as initially described by Fox et al., (2005) and Fransson et al., (2005), may be frequency dependent. Furthermore, studies comparing network connectivity between resting state and tasks tend to retain high frequencies, with the assumption that behaviourally relevant signals are in the higher ranges (Cole et al., 2014; Schultz and Cole, 2016; Cole et al., 2016). This is due to the fact that univariate analyses of task-based fMRI data typically employ highpass filters. Though this is a sensible intuition, a direct investigation of bandpass and highpass filtered datasets and the effect of filtering on DMN connectivity during tasks has not yet been performed.

The current study fills this gap in the literature by presenting novel evidence of higher frequency DMN connectivity and its relationship to behaviour. Data from resting state, a finger opposition task (blocked design) and a stop signal task (event-related design) were temporally preprocessed in two different ways, one using bandpass filtering ($0.009 < f < 0.08$) and one using highpass filtering ($0.009 < f < 0.25$). These tasks were selected to investigate how temporal filtering affects DMN connectivity during both block and event-related task designs. We hypothesized that the inclusion of high frequencies would alter connectivity patterns between DMN and DAN across behavioural state. Furthermore, we hypothesised that retaining high frequency fluctuations in the DMN would be associated with task performance.

2. Methods

2.1 Participants

This study was approved by the Cambridgeshire 2 Research Ethics Committee (LREC 08/H0308/246) and all participants gave written informed consent before testing. All participants were right handed, had no history of psychiatric or neurological disease, no history of drug or alcohol abuse, no contraindication to MRI scanning or severe claustrophobia, and were not taking medication that affect their physical or cognitive performance. Additional exclusion criteria required a score above 70 on the National Adult Reading Test (NART) and a score above 23 on the Mini Mental State Exam (MMSE). 22 healthy participants were included in the study (19-57 years old, mean = 35.0, standard deviation = 11.2, 9 females and 13 males). Participants had average scores of 117.1 (SD = 5.76) on the NART and 29.33 (SD = 0.85) on the MMSE.

2.2 Paradigm specifications

2.2.1 Resting State

Participants underwent a 5 minute resting state scan where they were instructed to stay still and keep their eyes closed.

2.2.2 Motor task

The motor task is a boxcar design, self-paced finger opposition paradigm with 5 alternating 30 second blocks of task and fixation (5 minutes total). Participants were instructed to touch their fingers with their right thumb, moving sequentially from the index to the little finger. They continued this process throughout the entire duration of the task block. The task block was initiated by participants seeing the word "move" on the screen, while fixation blocks started with participants seeing the word "rest".

2.2.3 Stop Signal Task

The Stop Signal Task (SST) is an event-related fMRI paradigm and has previously been described by Rubia et al. (2003; 2007). Briefly, an arrow is displayed on a computer screen (white on black background) that is facing either left or right. Participants are instructed to respond with their right index or middle fingers depending on the arrow direction (go trials).This task has a total of 240 trials including 200 go trials and 40 stop trials. There were a minimum of 3 and a maximum of 7 go trials between each stop trial.

The stimulus duration for go trials was 1000ms, while the stop trial stimulus duration was a minimum of 100ms and maximum of 300ms. In a subset of trials, the arrow is followed by another arrow pointing upwards (stop trials), indicating the participant should stop themselves from pressing a button. For the first stop trial, the interval between onset of the go trial and onset of the stop trial (i.e. stop signal delay; SSD) was 150ms. Stopping difficulty is manipulated across trials by a tracking algorithm described by Rubia et al. (2003) that is designed to alter the time interval between go and stop signals so that each participant succeeds in 50% of the stop trials. Successful inhibition resulted in the SSD to increase by 50ms, whereas unsuccessful inhibition resulted in SSD decreasing by 50ms. This ensures that each participant is working at the edge of their ability, resulting in a comparable level of difficulty between subjects. Of the four conditions included in this task (go success, go failure, stop success, stop failure), only go success trials were considered in this study. This is because we are interested in measuring task-related activity generally, not neural activity specific to stop inhibition. One subject was removed from the stop signal task because of excessive head motion during scanning, leaving 21 subjects in this group.

2.3 Data Acquisition

MRI data was obtained using a Siemens Trio 3T scanner (Erlangen, Germany) equipped with a 12-channel head matrix transmit-receive coil at the Wolfson Brain Imaging Centre at Addenbrooke's Hospital in Cambridge, UK. First, participants underwent a high resolution T1-weighted, magnetization-prepared 180 degree radio-frequency pulses and rapid gradient-echo (MPRAGE) structural scan (TR = 2300ms; TE = 2.98 ms; TA = 9.14 min; flip angle = 9°; field of view (FOV) read = 256mm; voxel size = 1.0 x 1.0 x 1.0mm, slices per slab = 176). The structural scan was followed by whole-brain echo planar imaging (EPI) for the resting-state, motor task and SST (TR = 2000ms; TE = 30ms; flip angle = 78°; FOV read = 192 mm; voxel size = 3.0 x 3.0 x 3.75mm; volumes = 160; slices per volume = 32). Other tasks were also completed by the participants (N-back, Tower of London and Rapid Visual Information Processing) and were presented in a randomised order. The motor task always followed the resting state scan and randomisation of the remaining tasks was used to avoid potential fatigue on any single

task. Portions of this data were used in previously published studies to address alternative experimental questions (Vatansever et al., 2015a, 2015b, 2016a, 2016b; Moreno-López et al., 2016).

2.4 Preprocessing

Preprocessing for resting state functional data and task functional data followed an identical pipeline described below.

2.4.1 Spatial Preprocessing

Spatial preprocessing for functional and structural images was performed using Statistical parametric Mapping (SPM) 8.0 (http://www.fil.ion.ucl.ac.uk/spm/) and MATLAB Version 2008a (http://www.mathworks.co.uk/products/matlab/). Weissenbacher et al. (2009) performed a comprehensive analysis of preprocessing step order and found the following order to be most optimal. 1) Slice timing correction, 2) Realignment, 3) Spatial normalization, 4) Smoothing, 5) Noise Signal removal. We deviated slightly from step 5 in that we used the anatomical CompCor method for removing noise signals (Behzadi et al., 2007). Otherwise we used the preprocessing step order they defined in their paper. For all functional scans, the first 5 volumes were removed to eliminate saturation effects and achieve steady state magnetization. Subsequently, functional data was slice-time adjusted and underwent motion correction using SPM realign. High resolution T1 structural images were co-registered with the mean EPI and segmented into grey matter, white matter and cerebrospinal fluid masks and were spatially normalized to Montreal Neurological Institute (MNI) space with a resolution of 2 x 2 x 2mm cubic voxels. (Ashburner & Friston, 2005). Transformation parameters were applied to motion corrected functional images that were then smoothed with a 6 mm FWHM Gaussian kernel.

2.4.2 Temporal filtering

To deal with physiological and movement-related noise, data underwent despiking with a hyperbolic tangent squashing function, followed by the anatomical CompCor (aCompCor) technique. aCompcor removes the first 5 principal components of the signal from white matter and cerebrospinal fluid masks, as well as the motion parameters and their first-order temporal derivatives and a linear detrending term

(Behzadi et al., 2007). aCompcor has been shown to effectively remove physiological noise components that would otherwise be aliased in to data sampled at the standard ~2s TR. This process was identical for both temporal filtering sets.

Each subjects' preprocessed functional images were then highpass (0.009 Hz < f < 0.25 Hz) and bandpass filtered (0.009 Hz < f < 0.08 Hz). 0.25 Hz was selected as the low-pass filter for the high-pass group because it is the Nyquist frequency for data acquired with a TR of 2. The Nyquist frequency is the highest reliably sampled frequency given the sampling rate of the data (i.e. Half the sampling rate). This resulted in two groups of functional images that were identical except that one was highpass filtered and the other was bandpass filtered. Temporal filtering was performed using a Fast Fourier Transform (FFT).

2.5 Obtaining Power Spectrum

We calculated the power spectrum at the single subject level using the Fast Fourier Transform implemented with MATLAB Version 2008a (http://www.mathworks.co.uk/products/matlab/). The frequency bands were restricted to signals between 0.009 and 0.25 Hz.

2.6 ROI Definition

ROIs were defined as 10mm spheres and centred at seven regions (Fox et al., 2005). Four of the regions made up the default mode network and included the posterior cingulate cortex/precuneus (PCC; -6, -52, 40), medial prefrontal cortex (mPFC; -1, 49, -5) and right (R Ang; 46, -70, 36) and left (L Ang; -46, -70, 36) angular gyri. As is standard in studies examining DMN connectivity, global connectivity of the PCC is reported. The remaining three ROIs made up the task-positive network and were centred in the intraparietal sulcus (IPS; -25, -57, 46), the frontal eye field region of the precentral sulcus (FEF; 25, -13, 50) and the middle temporal region (MT^{+}; -45, -69, 2). Seed based connectivity results from the IPS are also reported to show DAN connectivity. Spherical ROIs were created using the MarsBaR toolbox (http://marsbar.sourceforge.net).

2.7 ROI-to-Voxel Functional Connectivity

We calculated ROI-to-Voxel (seed based) connectivity from one ROI for both the DMN (PCC seed) and DAN (IPS seed) for each behavioural condition: 1) Resting-state, 2) Block Motor Task, 3) Event-related SST. Each analysis used two sets of the same functional data, with the only difference between the sets being the temporal filtering (highpass vs. bandpass filtering).

In the SST, functional connectivity was measured for events when subjects successfully completed a go trial (go-success). Go-success trials were used because a) they occurred more often than the other events (i.e. go-failure, stop-success, stop-failure) and b) we are interested in the general effects of bandpass filtering on an event-related design, not on stop inhibition specifically.

Both highpass and bandpass filtered images for resting state, motor task and SST were entered into the Conn toolbox (Whitfield-Gabrieli and Nieto-Castanon, 2012). The Conn Toolbox is a set of Matlab scripts for running functional connectivity analyses that utilizes SPM routines. This method computes temporal correlations between a region of interest (ROI) and all other brain voxels using a General Linear Model approach. Data from any subject moving more than half a voxel (> 1.5mm) during scanning was removed. A total of 22 datasets (for each temporal filtering group, N = 22 highpass; N = 22 bandpass) were included in rest and motor analysis. The SST included 21 datasets (N = 21 highpass; N = 21 bandpass). One subject was excluded from the SST due to excessive head motion during scanning.

Resting state, motor task and SST ROI-to-voxel parameter estimate (Beta coefficient) maps for each ROI in both bandpass and highpass datasets were calculated for each subject and entered into second level analyses using a one sample t-test in SPM. Age was entered as a confounding variable in all second level analyses. We report results that survived $p < 0.001$, uncorrected at the voxel level $p < 0.05$, FWE-corrected for multiple comparisons at the cluster level.

To identify statistical differences in connectivity maps for different filtering sets, resting state, motor task and SST seed-to-voxel parameter estimate (Beta coefficient) images for each ROI in both bandpass and highpass datasets were calculated for each subject and entered into second level analyses using paired t-tests in SPM. Age was

entered as a confounding variable in these second level analyses. Results were considered significant at voxel level ($p < 0.001$, uncorrected) and cluster level ($p < 0.05$, FWE-corrected for multiple comparisons).

2.8 ROI-to-ROI Functional Connectivity

We also directly compared connectivity between the seven ROIs (four for DMN and three for DAN) in the three behavioural states. We constructed 7x7 matrices of Fisher z-transformed bivariate correlation coefficients (Pearson's r) using the ROIs described above. A hierarchical clustering analysis that places functionally similar ROIs in either DMN or DAN domains was conducted to assess whether any region changed its network membership across behavioural state. All connections between ROIs were FWE corrected ($p < 0.05$) at the ROI and network levels using the Network Based Statistics (NBS) toolbox. This method uses non-parametric permutation testing of network intensity to identify which ROI-to-ROI functional connections were statistically significant (Zalesky et al., 2010).

2.9 Relating DMN connectivity with reaction time

Connectivity within the DMN was measured and correlated with reaction time in the go success trials for the stop signal task, with the aim of assessing the relationship between DMN connectivity and a measure of behavioural performance at the subject-level. This analysis involved averaging the edge strength (Pearson correlation coefficients normalised to z scores using the Fisher Transformation) between PCC and the three DMN nodes (mPFC, L Ang and R Ang). The final value is a measure of network wide correlations for each subject in the analysis. This step was performed for both highpass and bandpass filtered sets, resulting in two different groups (Highpass PCC-DMN Connectivity, Bandpass PCC-DMN Connectivity). These values were then correlated (Pearson's Correlation using R studio (https://www.rstudio.com/)) with each subject's reaction time score. An equivalent analysis was not carried out for the motor task because performance was not assessed during motor task beyond ascertaining visually that participants were carrying out the task.

3. Results

3.1 Effects of aCompCor and Temporal Filtering on BOLD Signal

The present study focused on understanding the role of high frequencies in DMN connectivity and their behavioural relevance. Figures 1(A-J) show the power spectrum (Fast Fourier Transform) from the average signal obtained from the grey matter mask of one subject used in the analysis. The top row panels (A, B, C) show the raw data, the middle row shows the effects of aCompCor preprocessing with a highpass filter (D, E, F), and the bottom row shows aCompCor preprocessing with a bandpass filter. (H, I, J). As expected, most of the power is contained within low frequencies (less than 0.08 Hz). However it is clear that some power is contained within higher frequencies as well, suggesting that potentially relevant activity is removed from functional connectivity analyses that implement bandpass filtering. To control for possible confounds, we used the Nyquist frequency as a lowpass filter in the highpass set to be sure all the signals analysed were reliably sampled. The following analyses aim to understand the functional and behavioural role of these high frequencies in relation to DMN connectivity.

3.2 The effects of high frequency fluctuations in network dynamics

Functional connectivity between the PCC ROI and all other voxels in the brain during rest (Figure 2A), motor task (Figure 2B) and stop signal task (Figure 2C) was used to measure DMN functional connectivity in both highpass and bandpass sets. Across all three states, both temporal filtering sets show similar positive functional connectivity with DMN regions including posterior cingulate/precuneus, medial prefrontal cortex, angular gyrus and medial temporal lobe structures. However a qualitative difference was observed between temporal filtering groups when examining anticorrelations between DMN and DAN. Both sets showed anticorrelations in anterior regions of the DAN, however the bandpass group showed greater anticorrelations with posterior DAN, most notably in bilateral inferior parietal cortex. This effect holds across all three behavioural states but is most prominent in the stop signal task. Functional connectivity between IPS and all other brain voxels was also measured for each behavioural state (Figures 3A-C). Connectivity between IPS and other DAN regions, including dorsolateral prefrontal cortex, anterior cingulate and right IPS, was observed. Again, we found a qualitative

increase in anticorrelations with DMN in bandpass filtered data compared to highpass filtered data, while subjects performed a task.

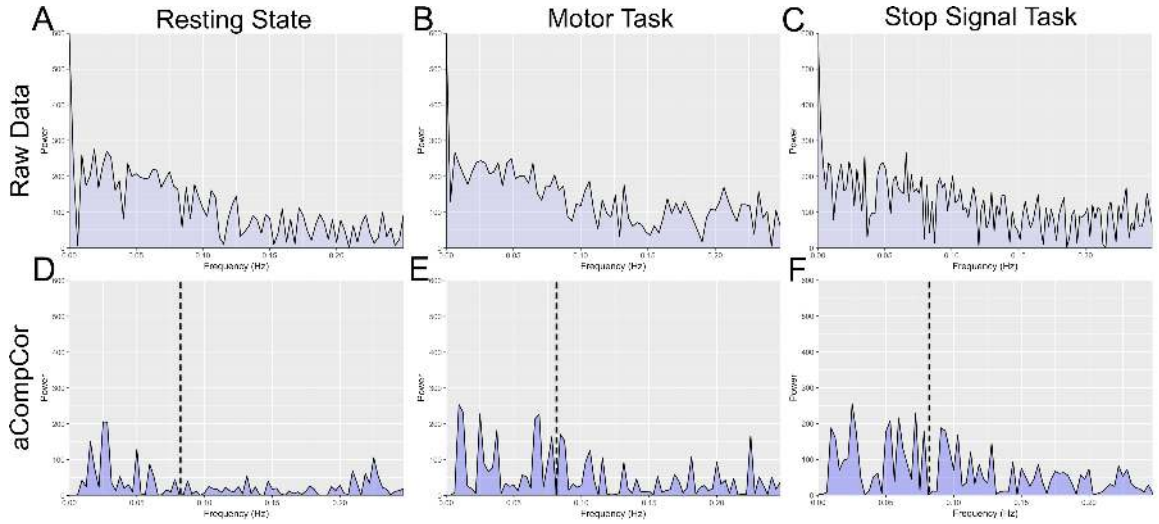

Figure 1: The Fast Fourier Transform (FFT) of the average grey matter signal from one subject for each task. The top row (A-C) shows the FFT of raw signal, before any temporal preprocessing. The bottom row (D-F) shows data that was denoised with aCompCor. The dotted line (located at 0.08 Hz) indicates where the lowpass filter in the bandpass filter group is applied. The highpass group contains frequencies above (to the right of) this dotted line (up to 0.25 Hz, i.e. the Nyquist frequency).

3.3 Differences in functional connectivity between highpass and bandpass sets

To examine whether the differences in functional connectivity between temporal filtering sets observed in the PCC were statistically significant, we used paired t-tests to compare connectivity maps for each condition (Figures 4A-C). We also measured functional connectivity from IPS to all other voxels to determine whether this effect is observed in a putatively dorsal attention network (Figures 5A-C). For the highpass > bandpass contrast, highlighted regions (in blue) represent a lower magnitude of anticorrelation in the highpass group compared to the bandpass group. For the bandpass > highpass contrast, highlighted regions (in red) represent a greater magnitude in correlation in the bandpass group compared to the highpass group. All results are significant at voxel level $p < 0.001$ (cluster $p < 0.05$ FWE-corrected).

At rest, the PCC showed less anticorrelation in highpass compared to bandpass in many regions of the DAN (Figure 4A). These include bilateral insula, premotor cortex and inferior parietal cortex, middle frontal gyrus, superior frontal gyrus, right supplementary motor area and several cerebellar regions. The PCC showed greater connectivity with DMN regions in the bandpass > highpass contrast, most notably the precuneus, mPFC, bilateral angular gyrus and middle temporal gyrus. For the motor task (Figure 4B), the PCC followed the same pattern as rest, with greater anticorrelation in the bandpass set for highpass > bandpass, and greater correlation in the bandpass group in the bandpass > highpass contrast. Greater anticorrelation in bandpass filtered data was observed in the bilateral insula, supramarginal gyrus (SMG), right supplementary motor area and right IFG. The bandpass > highpass contrast showed greater correlation between PCC and bilateral angular gyrus, mPFC, PCC, right IFG and right ITG for bandpass filtered data. In the stop signal task (Figure 4C), reduced anticorrelation was observed in the highpass group compared to the bandpass group in bilateral MFG, IPC, SFG, right MTG, left insula and right and left IOC. Increased correlation was seen in the bandpass group in the bandpass > highpass group in DMN regions, including left angular gyrus, bilateral PCC, mPFC and inferior frontal gyrus.

The IPS was less anticorrelated with several DMN regions in the highpass set (Figure 5A), including mPFC and right angular gyrus. There was also less anticorrelation with bilateral superior temporal gyrus and several motor regions, including right supplementary motor area and right precentral gyrus. The IPS showed greater correlation with DAN regions in the bandpass set for the bandpass > highpass contrast. Regions include the left inferior occipital cortex (IOC), left inferior parietal gyrus left inferior frontal cortex (IFG), left inferior parietal cortex (IPC), right precentral gyrus and right cerebellar crus II. For the motor task, the IPS (Figure 5B) showed less anticorrelation in the highpass set with DMN regions, including the mPFC, PCC and right angular gyrus. In the bandpass > highpass contrast, greater correlation is seen in the bandpass group between IPS and left MTG, right IFG, bilateral SFG, left anterior cingulate (ACC) and left superior occipital cortex. In the stop signal task, the IPS (Figure 5C) reduced connectivity in the highpass group in the highpass > bandpass contrast in several DMN regions including bilateral mPFC, precuneus, PCC, parahippocampal gyrus and right ITG.

For the bandpass > highpass contrast, IPS showed greater correlation in the bandpass group in DAN regions including left IFG, posterior ITG, superior parietal gyrus (SPG), MFG, IFG and right precentral gyrus.

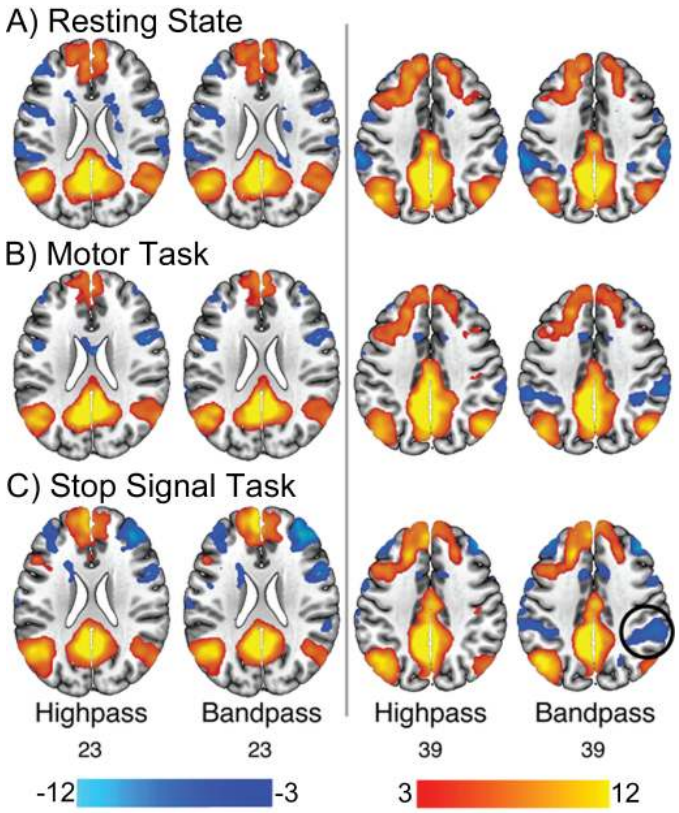

Figure 2: Whole brain connectivity analysis using PCC as a seed region. The differences between the two groups are most prominent in the right columns for the stop signal task (highlighted with a black circle). The first and third columns show highpass filtered data and the second and fourth columns show bandpass filtered data. A) shows PCC connectivity during resting state, B) shows PCC connectivity during the motor task and C) shows PCC connectivity during the stop signal task. Red maps are positive correlations (t values) and blue maps are anticorrelations. Numbers below the axial slices are MNI z coordinates.

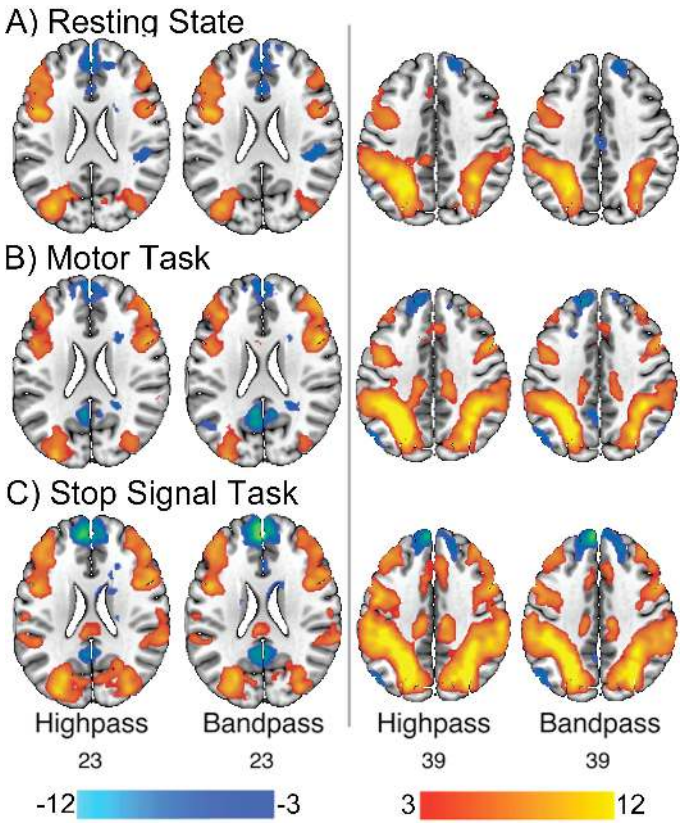

Figure 3: Whole brain connectivity analysis using IPS as a seed region. The first and third columns show highpass filtered data and the second and fourth columns show bandpass filtered data. A) shows IPS connectivity during resting state, B) shows IPS connectivity during the motor task and C) shows IPS connectivity during the stop signal task. Red maps are positive correlations (t values) and blue maps are anticorrelations. Numbers below the axial slices are MNI z coordinates.

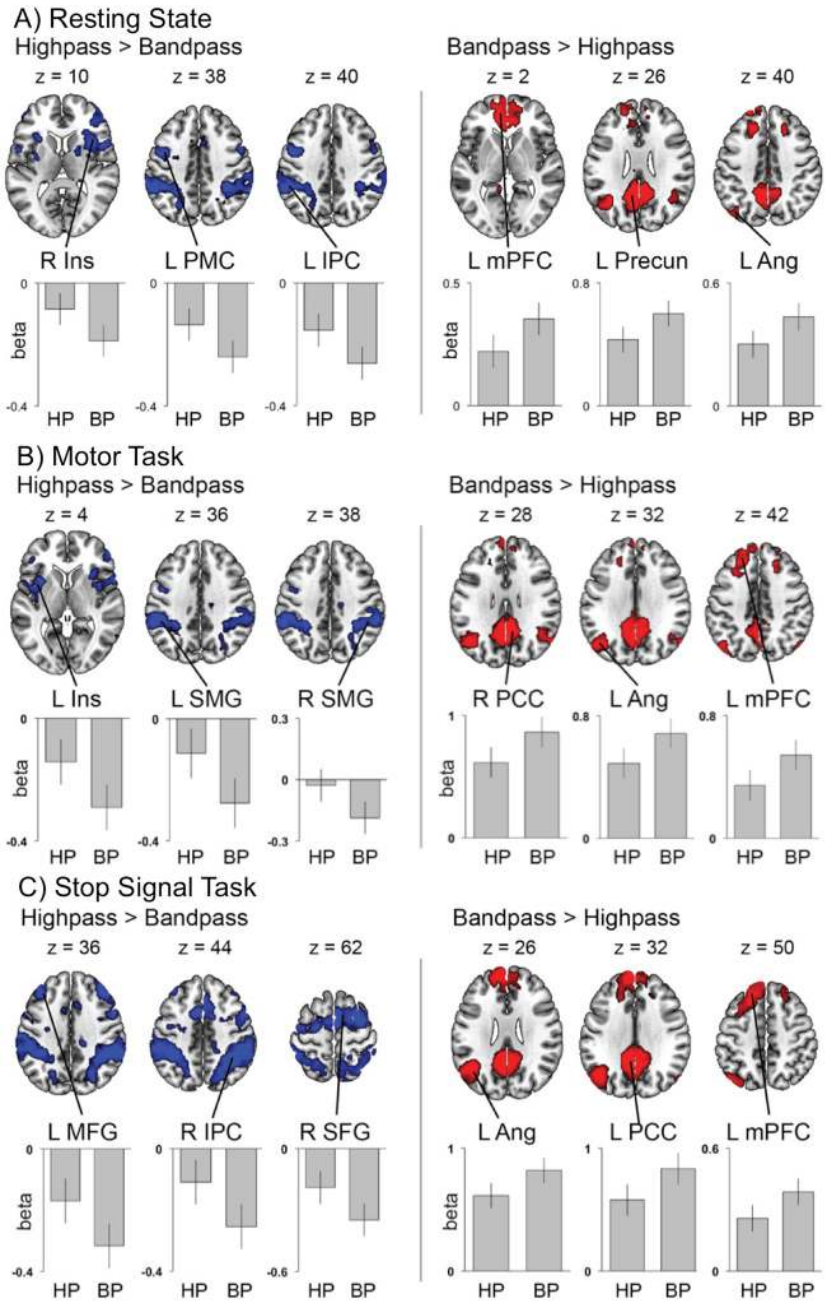

Figure 4: Statistical differences in PCC functional connectivity between highpass and bandpass filtered sets in resting state, motor task and stop signal task. Each subject's first level connectivity map for both filtering sets was entered into a paired t-test. All activations are statistically significant at $p < 0.001$ (cluster $p < 0.05$ FWE-corrected). The highpass greater than bandpass (blue regions) contrast is primarily located in TPN regions. The bandpass greater than highpass (red regions) contrast is primarily located in DMN regions.

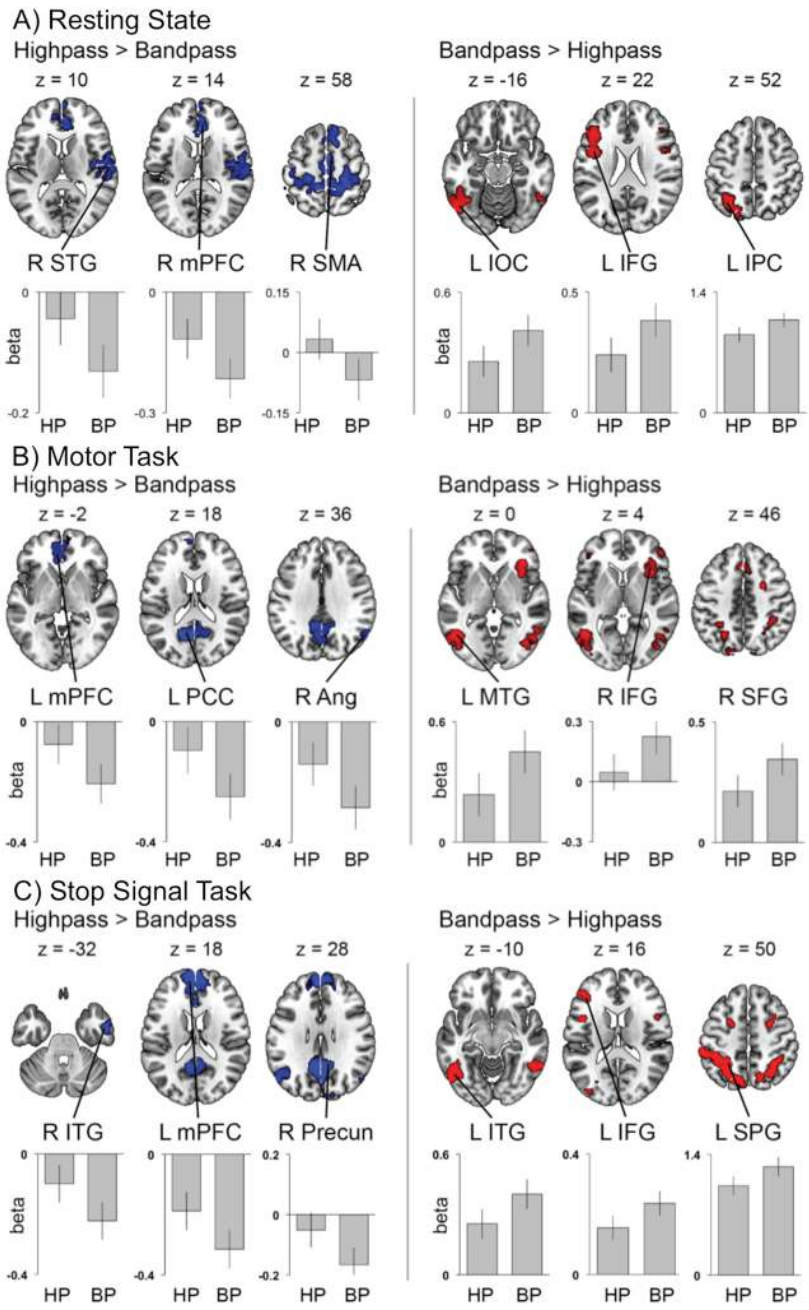

Figure 5: Statistical differences in IPS functional connectivity between highpass and bandpass filtered sets in resting state, motor task and stop signal task. Each subject's first level connectivity map for both filtering sets was entered into a paired t-test. All activations are statistically significant at $p < 0.001$ (cluster $p < 0.05$ FWE-corrected). The blue regions (highpass greater than bandpass) primarily shows reduced anticorrelations between IPS and DMN. The red regions (bandpass greater than highpass) primarily shows within TPN connectivity.

3.4 Task-related internetwork positive connections are dependent on the inclusion of high frequency fluctuations.

To directly measure the effect of behavioural task and high frequencies on network reconfiguration, we measured functional connectivity between 7 previously defined ROIs representing regions of the DMN (PCC, mPFC, L Ang, R Ang) and DAN (IPS, FEF, MT^{+}) (Fox et al., 2005). Our results show that within network connectivity is relatively stable regardless of temporal filtering used, however between network positive connectivity is reliant on the inclusion of high frequencies in the data. These results are represented as chord diagrams in Figure 6A-F.

First, using a hierarchical clustering algorithm, we show that nodes from both DMN and DAN were reliably allocated to their respective networks for each behavioural task in both temporal filtering sets, suggesting within network connectivity is relatively stable across behavioural task and temporal filtering set. Second, anticorrelations between networks exist for both temporal filtering sets, but are much more prominent in the bandpass set, complementing our ROI-to-Voxel results from the previous section. These anticorrelations also increase during task state for both temporal filtering sets. However, a positive, long-range connection between mPFC in the DMN and MT^{+} in the DAN is revealed only when high frequencies are included in the data. Crucially, this connection does not exist during resting state, and persists during both tasks, suggesting it is related to task engagement and not present due to high frequency noise, as that would likely be uniformly present across all three behavioural states. It is also not likely to have originated from residual motion related artefacts, as those tend to result in increased short-range and bilateral connections and decreased long-range, anterior-posterior connections (Murphy et al., 2013 Power et al., 2012). We additionally examined connectivity during the fixation block of the motor task and found no internetwork positive connectivity (data not shown).

3.5 Inclusion of high frequencies reveals task-related DMN connectivity

In addition to examining network reconfiguration in the context of a task, we were also interested in assessing the influence of high frequencies in DMN on task-related behavioural measures. To this end, we correlated connectivity within the DMN (edge

correlation strength of PCC to other DMN nodes) with reaction time in go success trials in the stop signal task for both highpass and band-pass filtered datasets. This analysis revealed a significant relationship with reaction time in the highpass group ($R^2 = 0.19$ r = -0.43, p = 0.046) (Figure 7A) but not the bandpass group ($R^2 = 0.084$ r = -0.29, p = 0.2) (Figure 7B), signifying that as within DMN connectivity increased, reaction time was faster. This could suggest that task related connectivity exists exclusively in high frequency fluctuations in the DMN, and that bandpass filtering removes these behaviourally relevant signals.

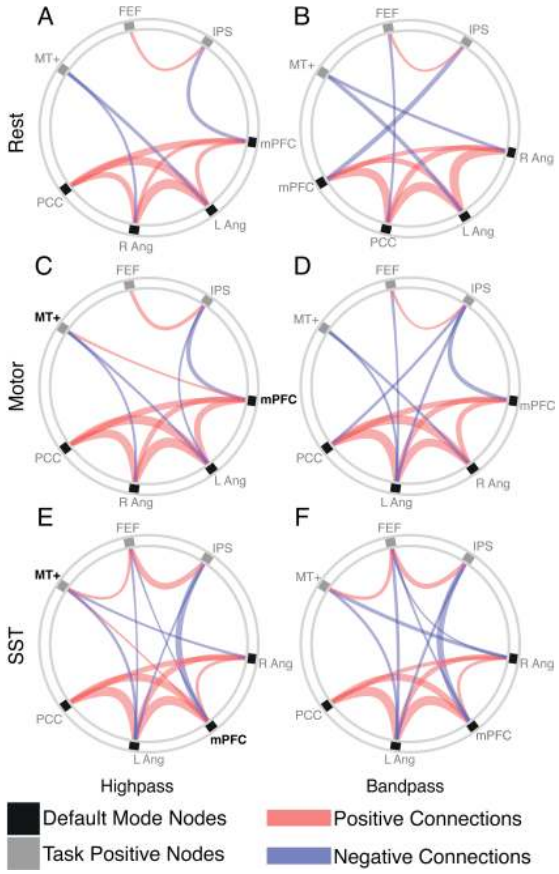

Figure 6: Chord diagrams showing ROI-to-ROI connectivity patterns between primary nodes in the DMN andTPN. C) and E) are of particular interest because they contain a positive connection between MT+ andmPFC, nodes (highlighted in bold) within the TPN and DMN respectively. All connections survived correctionfor multiple comparisons ($P < 0.05$, FWE-corrected) using the network based statistics toolbox (Zalesky etal., 2010). Node placement around the circle is determined by a hierarchical clustering algorithm, whichreliably separated each node into their respective networks for each analysis group. Red lines are positiveconnections and blue lines are negative connections. The strength of connectivity is proportional to thethickness of the line. Grey boxes show TPN nodes and black boxes show DMN Nodes. A) shows connectivityin the highpass set at rest. B) shows connectivity in the bandpass set at rest. C) shows connectivity in the highpass set during execution of a finger opposition motor task. D) shows connectivity in the bandpass set during execution of a finger opposition motor task. E) shows connectivity in the highpass set during go success trials of a stop signal task. F) shows connectivity in the bandpass set during go success trials of a stop signal task.

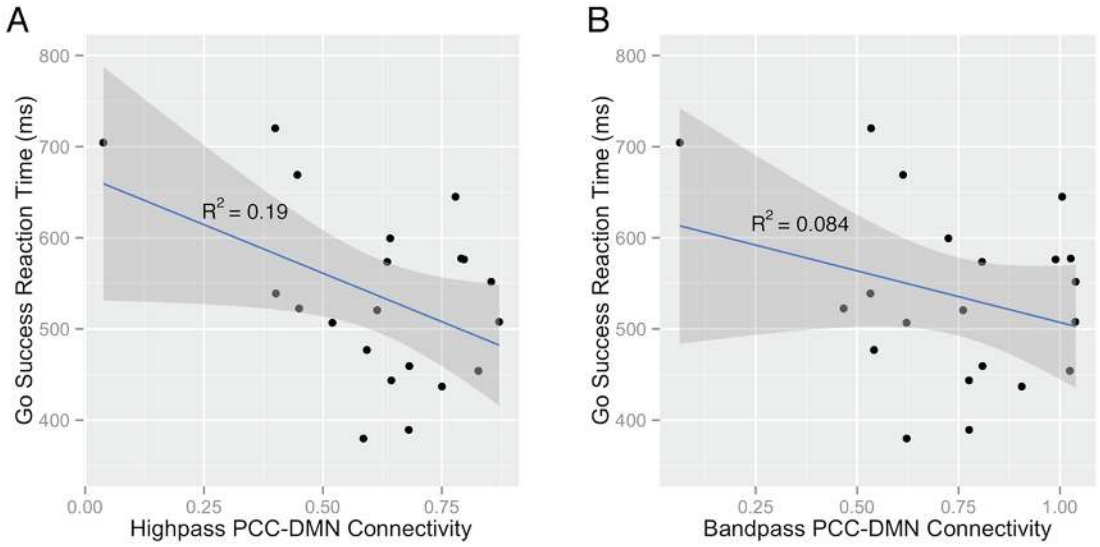

Figure 7: Pearson's Correlation of Go Success Reaction Time in the Stop Signal Task with DMN connectivity in highpass and bandpass sets. A) shows a significant negative correlation between highpass DMN connectivity with reaction time (R2 = 0.19, r = -0.438, p = 0.046), showing that reaction time is faster in subjects who have greater within-DMN connectivity. B) shows a non-significant relationship between bandpass DMN connectivity and reaction time (R2 = 0.08, r = -0.29, p = 0.2).

4. Discussion

Several recent studies have focused on measuring the role of high frequencies in functional connectivity during resting state scanning (Wu et al., 2008; Niazy et al., 2011; Boyacioglu et al., 2013; Gohel and Biswal, 2014; Kalcher et al., 2014; Chen and Glover, 2015; De Domenico et al., 2016; Lewis et al., 2016). At the same time, increasing evidence is suggesting that the DMN is not a "task-negative" network, but plays an active role in mediating a variety of cognitive processes (Seghier and Price, 2012; Spreng, 2012; Spreng et al., 2014; Vatansever et al., 2015a; Vatansever et al., 2015b; Crittendon et al., 2015; Vatansever et al., 2016). In an effort to bridge these two emerging lines of evidence the aim of the present study was to identify whether inclusion of high frequency fluctuations in fMRI data alter DMN connectivity patterns and whether these alterations are task relevant. To this end, we used fMRI data from three behavioural states (resting state, motor task, stop signal task) processed with either a bandpass (0.009 Hz < f < 0.08 Hz) or highpass (0.009 Hz < f < 0.25 Hz) filter. DMN connectivity was measured and

compared for each behavioural state and both filtering sets using ROI-to-Voxel and ROI-to-ROI connectivity. Using PCC as a seed region, we found that anticorrelations between PCC and posterior regions of the DAN were significantly reduced when high frequency fluctuations were included, an effect observed across all three behavioural states, though was most prominent in the event-related stop signal task. We also observed the inverse effect when measuring connectivity from IPS, a region of the DAN. Complementing our ROI-to-voxel result, we measured connectivity between DMN and DAN ROIs and observed stronger anticorrelations in the bandpass group across all three behavioural states, suggesting that between-network anticorrelations primarily fluctuate in low frequencies. Furthermore, we found that when high frequencies are included in the data, positive connectivity is observed between the mPFC and MT^{+}. Critically, this connection is only seen when subjects are engaged in a task and not during resting state. Our final analysis extended our initial findings to examine the behavioural relevance of within-DMN connectivity for individual subjects. Here we found that greater within-DMN positive connectivity predicted faster reaction times in the highpass set, but not the bandpass set. This shows that behaviourally relevant signals contained within the DMN exist at high frequencies, which are often removed in functional connectivity analyses attempting to establish the DMN's role in behaviour.

4.1 Within-network correlations and between network anticorrelations are most prominent in low frequency fluctuations

Our results confirm and expand upon previous observations that anticorrelations are present between DMN and DAN in low frequencies (Fox et al., 2005; Fransson 2005; Keller et al., 2013). We show that PCC anticorrelations are stronger in the bandpass set compared to the highpass set. Conversely, anticorrelations between IPS and regions of the DMN were also stronger in the bandpass set. Importantly we see this effect during all three behavioural states. These results show anticorrelations are greater at low frequencies when using seed regions from different networks, suggesting that this result is not specific to DMN regions.

We also observed greater within DMN connectivity in the bandpass set compared to the highpass set. It has been suggested that anticorrelations serve to segregate neuronal

processes that subserve opposite goals or competing representations (Fox et al., 2005). This relationship between DMN and DAN has been extensively explored, with many groups suggesting a dynamic set of processes wherein DMN is involved in internally directed, self-generated cognition and DAN involved in externally directed cognition (Andrews-Hanna et al., 2014). Further work has shown that DAN is actually comprised of multiple subnetworks, including the dorsal attention network (DAN), cingulo-opercular network (CON) and frontoparietal control network (FPCN) (Power et al., 2011). The DAN in particular has been shown to have an anticorrelated or antiphase relationship with DMN, while the FPCN is thought to play a mediating role between networks (Spreng et al., 2013). Importantly, the majority of studies focusing on the relationship between DMN and various DANs have applied bandpass filtering in the preprocessing stage, thus removing high frequencies from the statistical analysis. These anticorrelations have therefore been defined primarily in low frequencies. A likely interpretation could be that anticorrelations exist disproportionately at low frequencies, and that bandpass filtering allows for a sharper focus on this phenomenon. This is supported by significant evidence suggesting that anticorrelations are present in large scale networks independent of preprocessing techniques or experimental groups (Chai et al., 2012; Spreng et al., 2016).

4.2 Task-related internetwork connectivity is a high frequency phenomenon

In addition to finding that anticorrelations are behaviourally relevant and exist primarily in low frequencies, we provide two pieces of complementary evidence that suggest the DMN contains task related activity at frequencies higher than what are typically analysed in functional connectivity studies. First, we show that when directly comparing connectivity profiles between highpass and bandpass sets, a positive connection is observed between MT^{+} and mPFC only during tasks, not during rest. This connection is unlikely to have originated from noise, as one would expect noise to be uniform across all three fMRI datasets. Furthermore, it is not likely to be related to head motion because motion-related artefacts have been shown to increase short-range and bilateral connectivity and decrease long-range and anterior-posterior connectivity (Murphy et al., 2013, Power et al., 2012). The positive connection we observe is both

long-range and anterior-posterior. Second, we found that within-DMN connectivity reliably correlated with reaction time only in the highpass set. Previous studies have retained high frequencies when comparing task-related connectivity with resting state (He et al., 2013; Cole et al., 2014; Schultz and Cole, 2016; Cole et al., 2016), however to our knowledge, this is the first demonstration that the DMN displays task related connectivity only when high frequencies are included in the analysis. These results should be seen as a first step to elucidating network connectivity at higher frequency bands than usually considered as well as an investigation into the relationship between high frequency connectivity and behaviour. Further research with larger sample sizes and faster TRs (TR $\leq$ 0.5s) is necessary to draw more definitive conclusions

Several recent studies have shown that activity in large scale networks is not restricted to frequencies below 0.1 Hz. A previous study used a high sampling frequency (TR = 645 ms) to measure functional networks across 5 frequency bands at rest (Gohel and Biswal, 2014). They were able to identify well-established networks, including the DMN and several DANs in high frequency bands. They also observed significant interhemispheric connectivity across all frequency bands, suggesting functional integration between brain regions is a multi-band phenomenon. Concurrently, recent work has shown the DMN to be involved in a variety of cognitive tasks involving both internally and externally directed attentional processes (Spreng et al., 2013; Spreng et al., 2014; Vatansever et al., 2015a; 2015b; 2016a; 2016b;). In this context, our work expands upon both lines of research by finding task-related activity in the DMN in high frequencies. This work may also find application in the field of mind-wandering and unconstrained cognition. Likely due to its role in internally directed attention, the DMN has frequently been implicated in mind-wandering, however, a recent meta-analysis showed that several studies have reported connectivity between non-DMN regions during mind wandering (Fox et al., 2015). Another recent study used a novel experience sampling method to show that DAN activity increased when subjects reported controlling their attention, while DMN activity increased when subjects reported a state of internal mentation (Van Calster et al., 2016). These studies show that what has come to be known as resting state is a dynamic state where internetwork connectivity likely plays an important role, therefore mind-wandering and studies examining unconstrained cognition

should consider preserving high frequency fluctuations in their data.

There are many remaining questions regarding high frequency fluctuations and the DMN. The present study is limited in that it only measures connectivity using *a priori* defined sets of ROIs. One approach could be to examine whether different subregions of the DMN communicate with other networks at different frequencies (Leech et al., 2011; Bzdok et al., 2015). The use of data-driven approaches or multivariate analyses could extend this work. One such study by Crittenden et al. (2015) used multivoxel pattern analysis to show that DMN encodes task relevant information during performance of a task-switching behavioural paradigm. Though it was not the focus of the study, it should be mentioned that a low frequency bandpass filter was not applied to the data prior to statistical analysis. Dynamic connectivity methods are another important extension of this work. A recent study by Dixon et al. (2017) present a comprehensive analysis of DMN-DAN interactions across time, as well as between different cognitive states and DMN subsystems. (Dixon et al., 2017). Using dynamic functional connectivity to investigate the ever changing nature of the relationship between DMN and DAN, the authors show that anticorrelation between these networks is transient rather than persistent and that anticorrelation is most prominent with core DMN regions like the PCC, mPFC and angular gyri. Therefore another interesting extension of our work could be the investigation of high frequency connectivity in different DMN subsystems.

Previous work looking to measure high frequencies in fMRI during resting state have used frequency bands originally defined by electrophysiology studies (Penttonen and Buzsaki, 2003) that argue frequency bands oscillate following a natural logarithmic function. The current study did not use this definition of frequency bands because we were limited by the TR of 2s, meaning we could only reliably measure oscillations slower than the Nyquist frequency of 0.25 Hz. Future studies should use novel MR acquisition protocols, including multiplex and multiband EPI sequences (Feinberg et al., 2010; Larkman et all, 2006; Kalcher et al., 2014; Boubela et al., 2013; Boubela et al., 2014), that allow for faster TRs, and thus higher Nyquist frequencies, to further define the role of high frequencies during rest and task based functional connectivity. Using these acquisition protocols would also reduce the potential impact of physiological and motion related artifacts. A potential area of controversy in the functional connectivity literature

that applies to the current study is the use of denoising pipelines. We acknowledge that there are a variety of potential denoising methods that can influence functional connectivity results, including manual denoising using ICA (e.g. fsl_regfilt) and automated denoising methods that implement PCA (Kay et al., 2013) or ICA (Salimi-Khorshidi et al., 2014). We chose to use aCompCor because it has been shown to sufficiently remove noise when studying network interactions (Chai et al., 2012). However, a replication of these findings by researchers using alternative denoising pipelines is probably warranted before definitive conclusions on this matter are drawn.

There are two main conclusions that can be drawn from this study. First, we found that the inclusion of high frequencies in functional connectivity analyses results in differences in between network interactions. Second, this high frequency activity appears to be important particularly when examining connectivity during task performance. This is supported by two sets of results, both of which delineate the role of high frequencies in the DMN. First, we found differences in connectivity patterns while subjects perform an attentionally demanding task and second, DMN connectivity correlated with reaction time only when high frequencies are included. These results suggest that functional connectivity studies should also include high frequencies, especially when examining DMN connectivity during task execution.

Acknowledgements

The funding for this study was provided by the Evelyn Trust (RUAG/018). MC is funded by the Cambridge International Trust and the Howard Research Studentship at Sidney Sussex College, University of Cambridge. DKM was funded by the NIHR Cambridge Biomedical Centre (RCZB/004), and an NIHR Senior Investigator Award (RCZB/014) and EA Stamatakis was supported by the Stephen Erskine Fellowship Queens' College Cambridge. The authors thank the staff in the Wolfson Brain Imaging Centre (WBIC) at Addenbrooke's Hospital for their assistance in scanning.

References

1. Andrews-Hanna JR (2012) The brain's default network and its adaptive role in internal mentation. *The Neuroscientist* 18(3):251-70.
2. Andrews-Hanna JR, Smallwood J, Spreng RN (2014) The default network and self-generated thought: component processes, dynamic control, and clinical relevance. *Ann N Y Acad Sci* 1316:29-52.
3. Ashburner, J., & Friston, K. J. (2005). Unified segmentation. *Neuroimage*, 26(3), 839-851.
4. Behzadi Y, Restom K, Liau J Liu TT (2007) A Component Based Noise Correction Method (CompCor) for BOLD and Perfusion Based fMRI. *Neuroimage* 37(1): 90–101.
5. Birn RM, Smith MA, Jones TB, Bandettini PA (2008) The respiration response function: the temporal dynamics of fMRI signal fluctuations related to changes in respiration. *Neuroimage* 40(2):644-54.
6. Biswal B, Yetkin FZ, Haughton VM, Hyde JS (1995) Functional connectivity in the motor cortex of resting human brain using echo-planar MRI. *Magn Reson Med* 34(4):537-41.
7. Boubela RN, Kalcher K, Huf W, Kronnerwetter C, Filzmoser P, Moser E (2013) Beyond Noise: Using Temporal ICA to Extract Meaningful Information from High-Frequency fMRI Signal Fluctuations during Rest. *Front Hum Neurosci* 7:168
8. Boubela RN, Kalcher K, Nasel C, Moser E (2014) Scanning fast and slow: current limitations of 3 Tesla functional MRI and future potential. *Front Physics 2:00001.*
9. Boyacioglu R, Beckmann CF, Barth M (2013) An Investigation of RSN Frequency Spectra Using Ultra-Fast Generalized Inverse Imaging. *Front Hum Neurosci* 7:156.
10. Buckner RL, Andrews-Hanna JR, Schacter DL (2008) The brain's default network: anatomy, function, and relevance to disease. *Ann N Y Acad Sci* 1124:1-38
11. Buckner RL, Carroll DC (2006) Self-projection and the brain. *Trends Cogn Sci* 11(2):49-57.

12. Buffalo EA, Fries P, Landman R, Buschman TJ, Desimone R (2011) Laminar differences in gamma and alpha coherence in the ventral stream. *Proc Natl Acad Sci USA* 108(27):11262-7.
13. Buschman TJ, Miller EK (2007) Top-down versus bottom-up control of attention in the prefrontal and posterior parietal cortices. *Science* 315(5820):1860-2.
14. Bzdok D, Heeger A, Langner R, Laird AR, Fox PT, Palomero-Gallagher N, Vogt BA, Zilles K, Eickhoff SB (2015) Subspecialization in the human posterior medial cortex. *Neuroimage* 106: 55-71
15. Chai XJ, Castañón AN, Ongür D, Whitfield-Gabrieli S (2012) Anticorrelations in resting state networks without global signal regression. *Neuroimage* 59(2):1420-8
16. Chen JE, Glover GH (2015) BOLD fractional contribution to resting-state functional connectivity above 0.1 Hz. *Neuroimage* 107:207-18.
17. Cole, MW, Bassett, DS, Power, JD, Braver, TS, Petersen, SE (2014). Intrinsic and task-evoked network architectures of the human brain. *Neuron* 83, 238-251.
18. Cole, MW, Takuya, I, Bassett, DS, Schultz DH (2016). Activity flow over resting-state networks shapes cognitive task activations. *Nat Neurosci* 19: 1718-1726.
19. Crittenden BM, Mitchell DJ, Duncan J (2015) Recruitment of the default mode network during a demanding act of executive control. *Elife* 4:e06481.
20. Davey CE, Grayden DB, Egan GF, Johnston LA (2013) Filtering induces correlation in fMRI resting state data. *Neuroimage* 64:728-40.
21. De Domenico M, Sasai S, Arenas A (2016) Mapping Multiplex Hubs in Human Functional Brain Networks. *Front Neurosci* 10:326.
22. Deco G, Kringelbach ML (2016) Metastability and Coherence: Extending the Communication through Coherence Hypothesis Using A Whole-Brain Computational Perspective. *Trends Neurosci* 39(3):125-35.
23. Della-Maggiore V, Chau W, Peres-Neto PR, McIntosh AR (2002) An empirical comparison of SPM preprocessing parameters to the analysis of fMRI data. *Neuroimage* 17(1):19-28.
24. Dixon, ML, Andrews-Hanna, JR, Spreng RN, Irving ZC, Mills C, Girn M, & Christoff K (2017) Interactions between the default network and dorsal attention

network vary across default subsystems, time, and cognitive states. *Neuroimage* 147, 632-649.

25. Feinberg DA, Moeller S, Smith SM, Auerbach E, Ramanna S, Gunther M, Glasser MF, Miller KL, Ugurbil K, Yacoub E (2010) Multiplexed echo planar imaging for sub-second whole brain FMRI and fast diffusion imaging. *PLoS One* 5:e15710
26. Fox KC, Spreng RN, Ellamil M, Andrews-Hanna JR, Christoff K (2015) The wandering brain: Meta-analysis of functional neuroimaging studies of mind-wandering and related spontaneous thought processes. *Neuroimage*. 1(111). 611-621
27. Fox MD, Snyder AZ, Vincent JL, Corbetta M, Van Essen DC, Raichle ME (2005) The human brain is intrinsically organized into dynamic, anticorrelated functional networks. *Proc Natl Acad Sci USA* 102(27):9673-8.
28. Fransson P (2005) Spontaneous low-frequency BOLD signal fluctuations: an fMRI investigation of the resting-state default mode of brain function hypothesis.
29. Fries P (2005) A mechanism for cognitive dynamics: neuronal communication through neuronal coherence. *Trends Cogn Sci* 9(10):474-80.
30. Glover GH (1999) Deconvolution of impulse response in event-related BOLD fMRI. *Neuroimage* 9 (4):416–429.
31. Gohel SR, Biswal BB (2015) Functional integration between brain regions at rest occurs in multiple-frequency bands. *Brain Connect* 5(1):23-34.
32. Greicius MD, Krasnow B, Reiss AL, Menon V (2003) Functional connectivity in the resting brain: a network analysis of the default mode hypothesis. *Proc Natl Acad Sci USA* 100(1):253-8.
33. He, B.J. (2013). Spontaneous and task-evoked brain activity negatively interact. The Journal of neuroscience : the official journal of the Society for Neuroscience 33, 4672-4682.
34. Hennig J, Zhong K, Speck O (2007) MR-Encephalography: Fast multi-channel monitoring of brain physiology with magnetic resonance. *Neuroimage* 34(1):212-9.

35. Kalcher K, Boubela RN, Huf W, Bartova L, Kronnerwetter C, Derntl B, Pezawas L, Filzmoser P, Nasel C, Moser E (2014) The spectral diversity of resting-state fluctuations in the human brain. *PLoS One* 9(4):e93375.
36. Kay KN, Rokem A, Winawer J, Dougherty RF, Wandell BA (2013) GLMdenoise: a fast, automated technique for denoising task-based fMRI data. *Front Neurosci* 7:247
37. Keller JB, Hedden T, Thompson TW, Anteraper SA, Gabrieli JD, Whitfield-Gabrieli S (2015) Resting-state anticorrelations between medial and lateral prefrontal cortex: association with working memory, aging, and individual differences. *Cortex* 64:271-80.
38. Leech R, Kamourieh S, Beckmann CF, Sharp DJ (2011) Fractionating the default mode network: distinct contributions of the ventral and dorsal posterior cingulate cortex to cognitive control. *J Neurosci* 31(9): 3217-2.
39. Lewis LD, Setsompop K, Rosen BR, Polimeni JR (2016) Fast fMRI can detec oscillatory neural activity in humans. *Proc Natl Acad Sci USA* 113(43) 6679-6685.
40. Logothetis NK, Pauls J, Augath M, Trinath T, Oeltermann A (2001) Neurophysiological investigation of the basis of the fMRI signal. *Nature* 12;412(6843):150-7.
41. Mantini D, Perrucci MG, Del Gratta C, Romani GL, Corbetta M (2007) Electrophysiological signatures of resting state networks in the human brain. *Proc Natl Acad Sci USA* 104(32):13170-5
42. Mazoyer, B, Zago, L, Mellet, E, Bricogne, S, Etard, O, Houde, O, Crivello, F, Joliot M, Petit L, Tzourio-Mazoyer N (2001) Cortical networks for working memory and executive functions sustain the conscious resting state in man. *Brain Research Bulletin* 54(3): 287-98.
43. Meyer MC, van Oort ES, Barth M (2013) Electrophysiological correlation patterns of resting state networks in single subjects: a combined EEG-fMRI study. *Brain Topogr* 26(1):98-109.
44. Minzenberg MJ, Watrous AJ, Yoon JH, Ursu S, Carter CS (2008) Modafinil shifts human locus coeruleus to low-tonic, high-phasic activity during functional MRI. *Science* 322(5908):1700-2.

45. Murphy K, Birn RM, Bandettini PA (2013) Resting-state fMRI confounds and cleanup. *Neuroimage* 80:349-59.
46. Murphy K, Birn RM, Handwerker DA, Jones TB, Bandettini P (2009) The impact of global signal regression on resting state correlations: are anti-correlated networks introduced? *Neuroimage* 44(3):893-905
47. Niazy RK, Xie J, Miller K, Beckmann CF, Smith SM (2011) Spectral characteristics of resting state networks. *Prog Brain Res* 193:259-76.
48. Penttonen M, Buzsáki G (2003) Natural logarithmic relationship between brain oscillators. *Thalamus & Related Systems* 2:145-152.
49. Popa D, Popescu AT, Paré D (2009) Contrasting activity profile of two distributed cortical networks as a function of attentional demands. *J Neurosci* 29(4):1191-201.
50. Power JD, Cohen AL, Nelson SM, Wig GS, Barnes KA, Church JA, Vogel AC, Laumann TO, Miezin FM, Schlaggar BL, Petersen SE (2011) Functional network organization of the human brain. *Neuron* 72(4):665-78.
51. Power JD, Barnes KA, Snyder AZ, Schlaggar BL, Petersen SE. Spurious but systematic correlations in functional connectivity MRI networks arise from subject motion. *Neuroimage*. 2012;59:2142–2154.
52. Raichle ME, MacLeod AM, Snyder AZ, Powers WJ, Gusnard DA, Shulman GL (2001) A default mode of brain function. *Proc Natl Acad Sci USA* 98(2):676-82.
53. Rubia K, Smith AB, Brammer MJ, Taylor E, (2003) Right inferior prefrontal cortex mediates response inhibition while mesial prefrontal cortex is responsible for error detection. *Neuroimage*. 20, 351-358.
54. Rubia K, Smith AB, Taylor E, Brammer M (2007) Linear age-correlated functional development of right inferior fronto-striato-cerebellar networks during response inhibition and anterior cingulate during error-related processes. *Hum. Brain. Mapp*. 28, 1163-1177.
55. Salimi-Khorshidi G, Douaud G, Beckmann CF, Glasser MF, Griffanti L, Smith SM (2014) Automatic denoising of functional MRI data: Combining independent component analysis and hierarchical fusion of classifiers. *Neuroimage* 90 449-468
56. Schultz D.H., Cole, M.W. (2016) Higher Intelligence Is Associated with Less Task-Related Brain Network Reconfiguration. *J Neurosci* 36(33): 8551-8561.

57. Seghier ML, Price CJ (2012) Functional Heterogeneity within the Default Network during Semantic Processing and Speech Production. *Front Psychol* 3:281.
58. Shulman GL, Fiez JA, Corbetta M, Buckner RL, Miezin FM, Raichle ME, Petersen SE (1997) Common Blood Flow Changes across Visual Tasks: II. Decreases in Cerebral Cortex. *J Cogn Neurosci* 9(5):648-63.
59. Siegel M, Donner TH, Engel AK (2012) Spectral fingerprints of large-scale neuronal interactions. *Nat Rev Neurosci* 13(2):121-34.
60. Skudlarski P, Constable RT, Gore JC (1999) ROC analysis of statistical methods used in functional MRI: individual subjects. *Neuroimage* 9(3):311-29.
61. Spreng RN (2012) The fallacy of a "task-negative" network. *Front Psychol* 3:145.
62. Spreng RN, DuPre E, Selarka D, Garcia J, Gojkovic S, Mildner J, Luh WM, Turner GR (2014) Goal-congruent default network activity facilitates cognitive control. *J Neurosci* 34(42):14108-14
63. Spreng RN, Grady CL (2010) Patterns of brain activity supporting autobiographical memory, prospection, and theory of mind, and their relationship to the default mode network. *J Cogn Neurosci* 22(6):1112-23.
64. Spreng RN, Sepulcre J, Turner GR, Stevens WD, Schacter DL (2013) Intrinsic architecture underlying the relations among the default, dorsal attention, and frontoparietal control networks of the human brain. *J Cogn Neurosci* 25(1):74-86.
65. Spreng RN, Stevens WD, Viviano JD, Schacter DL (2016) Attenuated anticorrelation between the default and dorsal attention networks with aging: evidence from task and rest. *Neurobiol Aging* 45:149-60.
66. Val Calster L, D'Argembeau A, Salmon E, Peters F, Majerus S (2017) Fluctuations of Attentional Networks and Default Mode Network during the Resting State Reflect Variations in Cognitive States: Evidence from a Novel Resting-state Experience Sampling Method. *J Cogn Neurosci* 29(1): 95-113
67. Van Dijk KR, Hedden T, Venkataraman A, Evans KC, Lazar SW, Buckner RL (2010) Intrinsic functional connectivity as a tool for human connectomics: theory, properties, and optimization. *J Neurophysiol* 103(1):297-321.

68. Vatansever D, Menon DK, Manktelow AE, Sahakian BJ, Stamatakis EA (2015a) Default mode network connectivity during task execution. *Neuroimage* 122:96-104.
69. Vatansever D, Menon DK, Manktelow AE, Sahakian BJ, Stamatakis EA (2015b) Default Mode Dynamics for Global Functional Integration. *J Neurosci* 35(46):15254-62.
70. Vatansever D, Menon DK, Manktelow AE, Sahakian BJ, Stamatakis EA (2016a) Cogntive Flexibility: A Default Network and Basal Ganglia Connectivity Perspective. *Brain Connect* Apr;6(3):201-7
71. Vatansever D, Manktelow AE, Sahakian BJ, Menon DK, Stamatakis EA (2016b) Angular default mode network connectivity across working memory load. *Hum Brain Mapp* DOI: 10.1002/hbm.23341.
72. von Stein A, Chiang C, König P (2000) Top-down processing mediated by interareal synchronization. *Proc Natl Acad Sci USA* 97(26):14748-53.
73. Weissenbacher A, Kasess C, Gerstl F, Lanzenberger R, Moser E, Windischberger C (2009) Correlations and anticorrelations in resting-state functional connectivity MRI: a quantitative comparison of preprocessing strategies. *Neuroimage* 47(4) 1408-1416
74. Whitfield-Gabrieli S, Nieto-Castanon A. (2012) Conn: a functional connectivity toolbox for correlated and anticorrelated brain networks. *Brain Conenct* 2(3): 125-41.
75. Wu CW, Gu H, Lu H, Stein EA, Chen JH, Yang Y (2008) Frequency specificity of functional connectivity in brain networks. *Neuroimage* 42(3):1047-55.
76. Zahneisen B, Grotz T, Lee KJ, Ohlendorf S, Reisert M, Zaitsev M, Hennig J (2011) Three-dimensional MR-encephalography: fast volumetric brain imaging using rosette trajectories. *Magn Reson Med* 65:1260–1268
77. Zalesky A, Fornito A, Bullmore ET (2010) Network-based statistic: identifying differences in brain networks. *Neuroimage* 53(4):1197-207.